

## Electromagnetic response of anisotropic superconductors

Karol I. Wysokiński and Tadeusz Domański

*Institute of Physics, Maria Curie-Skłodowska University, 20-031 Lublin, Poland*

(Received 15 July 1991)

We present a quantitative analysis of the ac electromagnetic properties of two-dimensional superconductors with an anisotropic energy gap and short coherence length. The mean-free path  $l$ , frequency  $f$ , and temperature  $T$  dependencies of surface impedance and complex conductivity have been discussed for the microwave and optical regions. The effect of the gap anisotropy has a strong influence on the calculated parameters. Some results seem to agree with puzzling experimental data on high- $T_c$  materials, thus offering a possibility of an alternative interpretation.

### I. INTRODUCTION

Finite-frequency electromagnetic properties reflecting the dynamics of carriers involved in superconductivity may play a central role in establishing the validity of any theoretically proposed model. BCS theory,<sup>1</sup> although based on schematic interactions, successfully describes—as calculated by Mattis and Bardeen<sup>2</sup>—the electrodynamics of conventional, low-temperature superconductors. It seems not to be so successful in describing the recently discovered high-temperature superconducting (HTS) copper oxides<sup>3</sup>.

Recently the electromagnetic properties of HTS have been intensively studied both theoretically<sup>4–12</sup> and experimentally.<sup>13–27</sup> The early experimental data on ceramics scattered widely from sample to sample and it was not obvious whether the observed behavior reflected the intrinsic characteristics of materials. The progress in technology resulted in the convergence of the data obtained by different groups. In spite of that, the interpretation problems still remain since the data do not always look like they should for a BCS superconductor; this leads to different proposals regarding the mechanism of superconductivity and the phenomenology of carrier dynamics.

The only way to overcome the interpretation ambiguities is to perform the theoretical analysis in models that take into account various peculiarities of the materials and carefully study their influence on the experimentally accessible parameters.

The BCS assumption of instantaneous interactions has been relaxed in Eliashberg theory.<sup>28</sup> The corresponding calculations of electromagnetic properties have been performed both for conventional<sup>29</sup> as well as high-temperature<sup>12,30,31</sup> superconductors.

The HTS are extremely unusual metals. They possess layered structure with conducting Cu-O planes, low carrier concentration, very short coherence length  $\xi$ , and large field penetration depth  $\lambda$ ; they are also quite disordered with mean-free path  $l$  of the order of 100 Å, etc.

Though it would be equally important to consider all the characteristic features of high- $T_c$  cuprate superconductors, the complexity of the materials, unknown values of interactions, and their role in superconductivity makes the theoretical analysis nontrivial. In this work we will concentrate on the study of the finite-frequency elec-

tromagnetic response of two-dimensional superconductors with an anisotropic energy gap and finite mean-free path.

The strong gap anisotropy with nodes at lines or points has been invoked for the interpretation of electronic Raman light scattering.<sup>32</sup>

Anisotropy or variations of the gap  $\Delta(\mathbf{k})$  around the Fermi line refers here to the crystal symmetry in  $ab$  plane of copper-oxide superconductors. Instead of estimating  $\Delta(\mathbf{k})$  in an anisotropic model, we introduce here the function  $\Delta(\mathbf{k})$  in a form consistent with the lattice symmetry. A simple parametrization

$$\Delta(\mathbf{k}) = \Delta_0 + \Delta_1 \cos(4\phi), \quad (1)$$

where  $\phi$  is the azimuthal angle of  $\mathbf{k}$  in  $ab$  plane, has been previously suggested by Mahan.<sup>33</sup> It gives quite interesting tunneling current characteristics,<sup>33,34</sup> which seem to be consistent with experimental data. The parametrization (1) allows the study of the gap which vanishes at some points of the Fermi line. It happens for  $|\Delta_0| = |\Delta_1|$ . We will study here the opposite case of anisotropic, but never vanishing, gap.

The organization of the paper is as follows: In Sec. II, we briefly recapitulate theoretical approach and the relations between measured quantities and theoretical parameters. The results of numerical calculations compared, where appropriate, with experimental data are presented in Sec. III. We end in Sec. IV with conclusions.

### II. ELECTROMAGNETIC RESPONSE KERNEL OF ANISOTROPIC SUPERCONDUCTOR

To obtain all the electromagnetic properties of a two-dimensional superconducting system, one investigates the so-called response kernel  $K(\mathbf{q}, \omega)$ . This function describes the current density induced by the external electromagnetic field  $\mathbf{A}(\mathbf{r}, t)$ . In a real layered copper-oxide superconductor, the Josephson coupling between adjacent sheets makes the system effectively three dimensional and may lead to a nonzero  $c$  component of the current  $\mathbf{j}$ . In this work, as a zeroth-order approximation we neglect the possible coupling between planes. The huge transport anisotropy observed<sup>37</sup> in high- $T_c$  superconduc-

tors justifies this assumption. The measurements show metalliclike conductivity in the  $ab$  plane and semiconducting one along the  $c$  axis implying the existence of the gap in the single-particle spectrum for motion in the  $c$  direction. The present analysis should thus be valid for both frequency and temperature small in comparison with that gap.

The vector potential  $\mathbf{A}$  is taken here in the Lorentz gauge,  $\text{div } \mathbf{A} = 0$ , and assumed to lie in the  $ab$  plane. The relation between Fourier components of  $\mathbf{j}$  and  $\mathbf{A}$  reads<sup>35</sup>

$$\mathbf{j}(\mathbf{q}, \omega) = -K(\mathbf{q}, \omega) \mathbf{A}(\mathbf{q}, \omega). \quad (2)$$

We are mainly interested in strong type-II superconductors with coherence lengths  $\xi$  much smaller than their penetration depth  $\lambda$  and mean-free path  $l$ . Under such circumstances, the electrodynamics is local<sup>35</sup> and it is enough to consider the  $\mathbf{q} \rightarrow 0$  limit.

The linear response theory leads to the following expression for the kernel  $\mathbf{K}(\omega)$  in terms of Green's functions:

$$\mathbf{K}(i\omega) = \frac{ne^2}{2m} \left[ 1 + \frac{2k_B T m}{n} \sum_{n=-\infty}^{\infty} \int \frac{d^2\mathbf{k}}{(2\pi)^2} v_x^2(\mathbf{k}) [G(\mathbf{k}, i\omega + i\omega_n) G(\mathbf{k}, i\omega_n) + F(\mathbf{k}, i\omega_n) F(\mathbf{k}, i\omega + i\omega_n)] \right]. \quad (3)$$

$G$  and  $F$  are the impurity-averaged Green's functions,<sup>36</sup>

$$G(\mathbf{k}, i\omega_n) = \frac{i\bar{\omega}_n - \xi_k}{(i\bar{\omega}_n)^2 - \xi_k^2 - |\bar{\Delta}(\phi)|^2}, \quad (4)$$

$$F(\mathbf{k}, i\omega_n) = \frac{\bar{\Delta}(\phi)}{(i\bar{\omega}_n)^2 - \xi_k^2 - |\bar{\Delta}(\phi)|^2},$$

with  $\xi_k = \varepsilon_k - \mu$ ,  $1/\tau$  being a scattering rate,  $v_x(\mathbf{k}) = (1/\hbar)(\partial\varepsilon_k/\partial k_x)$  the velocity, and

$$\bar{\omega} = \omega \left[ 1 + \frac{1}{2\tau} \frac{1}{\sqrt{\omega^2 + \Delta(\phi)^2}} \right], \quad (5)$$

$$\bar{\Delta}(\phi) = \Delta(\phi) \left[ 1 + \frac{1}{2\tau} \frac{1}{\sqrt{\omega^2 + \Delta(\phi)^2}} \right].$$

The relaxation time  $\tau$  describes the effects connected with the scattering on the static centers like vacancies, impurities, etc. We do not consider the interaction of the electromagnetic wave with moving impurities.

Performing a summation over Matsubara frequencies  $\omega_n = (2n+1)\pi k_B T$  and integrating over the two-dimensional  $\mathbf{k}$  vector, we arrive at the following formula for the response function:

$$\begin{aligned} K(\omega) = \frac{ne^2}{2m} \int_0^{2\pi} d\phi \frac{\sin^2(\phi)}{(2\pi)^2} & \left[ \int_{\Delta(\phi) - \hbar\omega}^{\Delta(\phi)} dy [1 - 2f(y + \hbar\omega)] \left[ \frac{g(y) + 1}{\varepsilon_2 - \varepsilon_1 + i\hbar/\tau} - \frac{g(y) - 1}{\varepsilon_2 + \varepsilon_1 - i\hbar/\tau} \right] \right. \\ & + \int_{\Delta(\phi)}^{\infty} dy [1 - 2f(y + \hbar\omega)] \left[ \frac{1 - g(y)}{\varepsilon_2 + \varepsilon_1 - i\hbar/\tau} + \frac{g(y) + 1}{\varepsilon_2 - \varepsilon_1 + i\hbar/\tau} \right] \\ & \left. - \int_{\Delta(\phi)}^{\infty} dy [1 - 2f(y)] \left[ \frac{g(y) - 1}{\varepsilon_2 + \varepsilon_1 + i\hbar/\tau} + \frac{g(y) + 1}{\varepsilon_2 - \varepsilon_1 + i\hbar/\tau} \right] \right] \quad (6) \end{aligned}$$

with

$$\varepsilon_1 = \begin{cases} \text{sgn}(y) \sqrt{y^2 - \Delta^2(\phi)} & \text{for } |y| > \Delta(\phi), \\ -i\sqrt{\Delta^2(\phi) - y^2} & \text{otherwise,} \end{cases} \quad (7)$$

$$\varepsilon_2 = \sqrt{(y + \hbar\omega)^2 - \Delta^2(\phi)},$$

$$g(y) = \frac{y(y + \hbar\omega) + \Delta^2(\phi)}{\varepsilon_1 \varepsilon_2}. \quad (7')$$

Here  $n$  is the density of electrons,  $m$  is the effective mass, and  $f(y)$  denotes the usual Fermi-Dirac function  $[\exp(y/k_B T) + 1]^{-1}$ . For the isotropic energy gap  $\Delta_0$ , expression (6) reduces to the standard result.<sup>35</sup> In deriv-

ing Eq.(6), we have neglected a variation of the term  $v_x^2(\mathbf{k})$  and replaced it by a constant  $\frac{1}{2}v_F^2$ . In view of the crude character of our model, this should not be a serious approximation.

Once we know the response function  $K(\omega)$ , we easily get complex conductivity  $\sigma_c = \sigma_1 + i\sigma_2$ , surface impedance  $Z(\omega)$ , penetration depth  $\lambda$ , and other parameters.<sup>35</sup> The relation

$$\sigma_c(\omega) = \frac{i}{\omega} K(\omega) \quad (8)$$

connects the response function with complex conductivity. In the London limit  $\xi \ll \lambda$ , the surface impedance

$$Z(\omega) = \frac{E(0)}{H(0)} \quad (9)$$

becomes equal to

$$Z(\omega) = i\omega\lambda(\omega) = \frac{i\omega}{\sqrt{K(\omega)}}, \quad (9a)$$

where  $\lambda(\omega)$  is penetration depth.

### III. RESULTS FOR TWO-DIMENSIONAL SUPERCONDUCTOR WITH ANISOTROPIC ENERGY GAP

Numerical calculations of penetration depth, complex conductivity, and surface impedance as a function of  $\omega$ ,  $T$ , and  $l$  will be discussed in this section for a number of  $\Delta_1$  values. For  $\Delta_1=0$  we get the results for the isotropic energy gap presented previously.<sup>5</sup> They will be shown here by dashed lines. It turns out that gap anisotropy modifies some of the dependencies quite strongly, making them look similar to that observed experimentally.

Here it is a good place to remind the reader of at least some of the previous work on electromagnetic properties of anisotropic three-dimensional superconductors. On the experimental side, let us mention early measurements<sup>38</sup> of surface resistance showing an effect of gap anisotropy and subsequent theoretical analysis by Clem.<sup>39</sup> Some of our results obtained for the two-dimensional system resemble those of Clem.<sup>39</sup>

#### A. Mean-free-path dependence

The dependence of the real part of conductivity in the superconducting state on mean-free path  $l$  is shown in Fig. 1.  $\sigma_1$  is normalized to  $\sigma_N = ne^2/2m\omega$ , which expresses the normal-state conductivity of the pure sys-

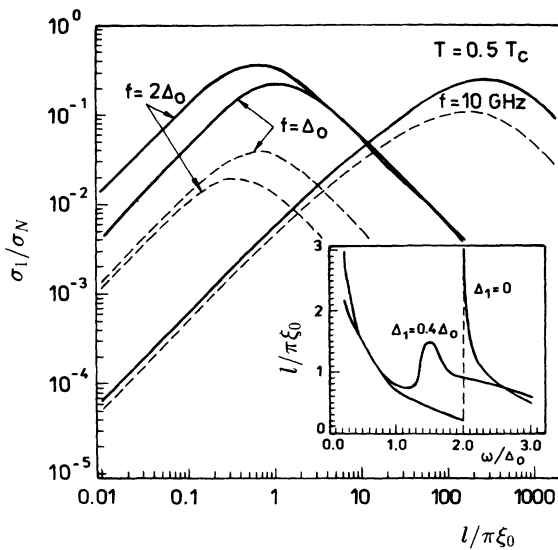


FIG. 1. Mean-free-path  $l$  dependence of the real part of conductivity  $\sigma_1$  for three frequencies: 10 GHz,  $\Delta_0$ , and  $2\Delta_0$ . The conductivity  $\sigma_1$  is normalized to  $\sigma_N = ne^2/2m\omega$  and the mean-free path  $l$  to  $\pi\xi_0$ . The inset shows the trajectory of maximum value of  $\sigma_1$  in  $(l, \omega)$  parameter space.

tem  $l \rightarrow \infty$ . We plot characteristics for two frequency regions, low frequencies (here 10 GHz) and the infrared region (here  $\hbar\omega = \Delta_0, 2\Delta_0$ ). We observe a slight shift of  $\sigma_1$  values when the isotropic energy gap (dashed lines) is replaced by anisotropic  $\Delta(\phi)$  (solid lines). This effect is large for frequencies near  $2\Delta_0$ . The pair-breaking mechanism leading to a sharp increase of  $\sigma_1$  in the pure system sets in at lower  $\omega$  in the anisotropic case.

The inset to Fig. 1 shows the position of the  $\sigma_1$  maximum in  $l$  and  $\omega$  space. In cleaner systems (long  $l$ ), the maximum of  $\sigma_1$  is observed at lower frequencies. There is, however, discontinuity of  $\sigma_1$  at  $\hbar\omega = 2\Delta_0$  for isotropic gap materials. The anisotropy smoothes the mentioned curve and makes it continuous.

We do not discuss  $\sigma_2$  dependence on  $l$  because it remains almost the same for isotropic and anisotropic gap material in the wide range of  $l$  values. In consequence, the imaginary part  $X_s$  of the surface impedance  $Z_s = R_s + iX_s$  is not influenced by the gap anisotropy.

Contrary to that, some interesting effects are observed in  $R_s$  dependence on  $l$  as shown in Fig. 2. Here anisotropy causes an increase of the resistance at frequencies 10 GHz, 100 GHz, and  $\omega = \Delta_0$ , but a slight decrease at the highest studied frequency  $\omega = 3\Delta_0$ . The data presented in Figs. 1 and 2 were obtained for temperature  $T = 0.5T_c$ , although similar behavior is observed at other temperatures.

#### B. Temperature dependence

When studying the temperature dependence one needs to know the temperature dependence of the gap function. In our calculations we used a typical BCS-like temperature dependence of the energy gap. We assumed that both  $\Delta_0$  and  $\Delta_1$  do depend on  $T$  in the same manner. Thus, we have

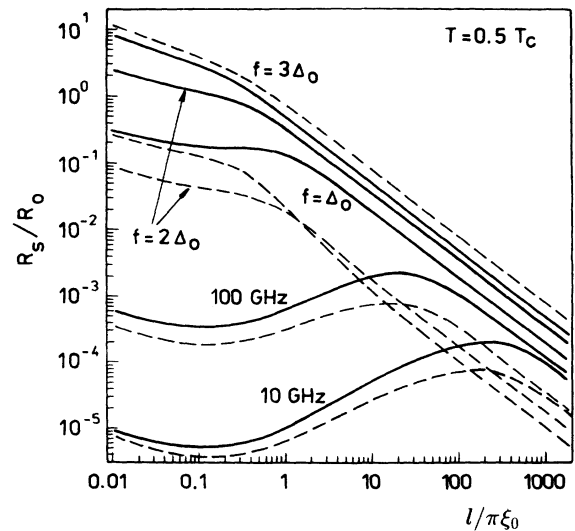


FIG. 2. Mean-free-path  $l$  dependence of the surface resistance  $R_s$  normalized to  $R_0 = (2m\mu_0/ne^2)^{1/2}(k_B T_c/\hbar)$ . The dashed lines refer to the isotropic energy gap and the solid lines refer to anisotropic one with  $\Delta_1/\Delta_0 = 0.8$ .

$$\Delta = \Delta_0(T)[1 + d_1 \cos(4\phi)], \quad (10)$$

where  $d_1 = \Delta_1/\Delta_0$  is a  $T$ -independent factor characterizing gap anisotropy.

The anisotropy, as expected, has a pronounced effect on the temperature dependence of surface resistance. This is illustrated in Figs. 3(a) and 3(b) at low frequencies and in Fig. 4 even more drastically at higher frequency. At low frequencies (Fig. 3) the surface resistance depends exponentially on  $T$  in region near zero and in the region near  $T_c$ . In between,  $R_s$  is a somewhat weaker function of temperature and this seems to be consistent with experimental data,<sup>24</sup> denoted by open circles in Fig. 3(b). Isotropic gaps lead to stronger temperature dependence.

At higher frequencies, e.g.,  $\hbar\omega = \Delta_0$ , the anisotropy when strong enough may lead (Fig. 4) to temperature-

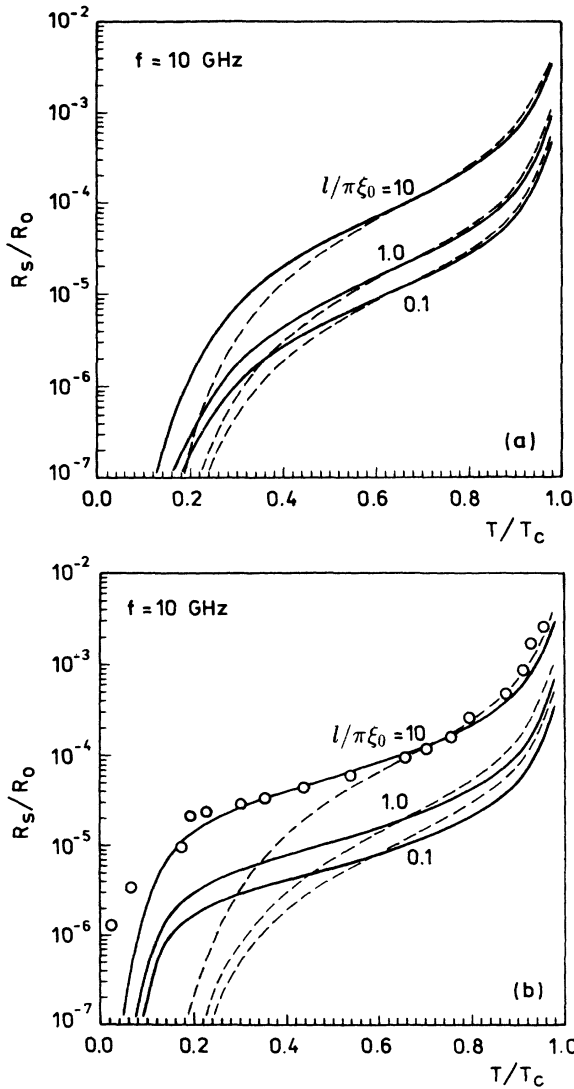


FIG. 3. Surface resistance  $R_s$  as a function of temperature  $T/T_c$  for frequency equal to 10 GHz and for three values of mean-free path, as indicated. The dashed curves refer to isotropic energy gap and the solid lines to anisotropic energy gap with (a)  $\Delta_1/\Delta_0=0.4$ , (b)  $\Delta_1/\Delta_0=0.8$ . The open circles represent the experimental data from Ref. 25.

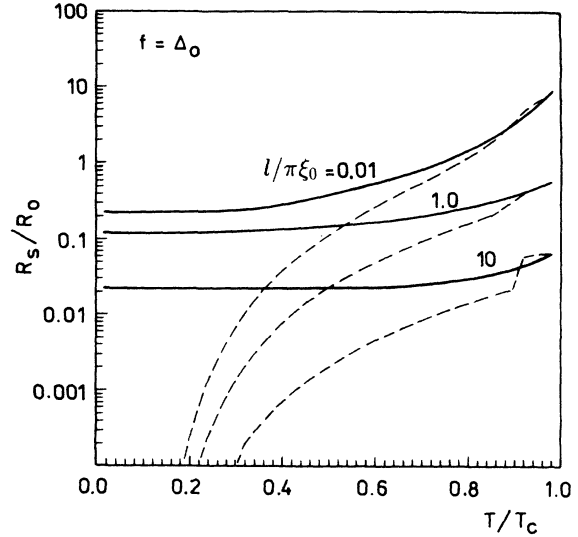


FIG. 4. The same as in Fig. 3(b) except that frequency  $f = \Delta_0$ .

independent (at low  $T$ ) and fairly large values of  $R_s$ . This kind of behavior can easily be understood on physical grounds. For a given value of the zero-temperature energy gap  $\Delta_0$ , the pair breaking is much more effective in systems with anisotropic gaps for which  $\Delta_1 \neq 0$ .

### C. Frequency dependence

Figures 5–8 show the dependence of surface resistance and the real part of conductivity on frequency expressed in  $\Delta_0$  units. The dashed lines refer to the isotropic energy gap and the solid ones to the anisotropic  $\Delta$  with  $\Delta_1/\Delta_0=0.4$  or  $0.8$ . We have shown the surface resistance  $R_s$  versus  $\omega = 2\pi f$  at different temperatures and for

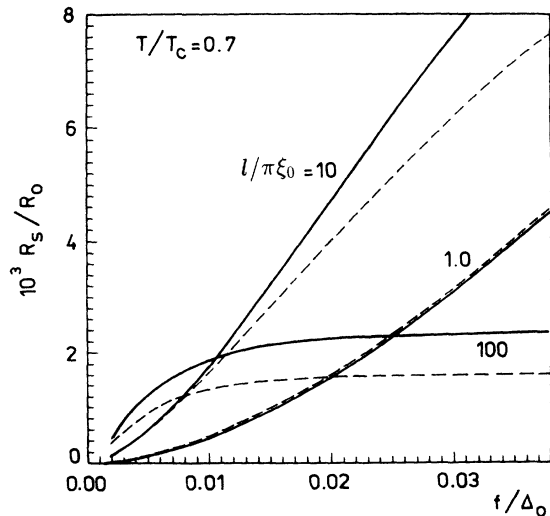


FIG. 5. Normalized surface resistance  $R_s$  as a function of frequency in the microwave region. The dashed lines refer to isotropic energy gap and the solid ones to anisotropic energy gap with  $\Delta_1/\Delta_0=0.8$ . Temperature is taken to be equal to  $0.7T_c$ .

various values of the mean-free path  $l$ . The surface reactance as well as imaginary part of the conductivity does not change appreciably when compared to isotropic gap systems.

Few results are worth noticing from Fig. 5 and similar results (not shown) calculated at different temperatures. First is that increase of temperature leads to increase of the magnitude of surface resistance as it should. The effect of anisotropy (in this case,  $d_1=0.8$ ) is weaker at higher temperatures. The mean-free path is an important parameter as the shape of  $R_s(\omega)$  changes from convex to concave with decreasing  $l$ .

At very low frequencies, from 0.1 GHz to hundreds GHz, and at small values of the reduced temperature  $t=T/T_c$ , many experimental data<sup>25</sup> point out at the quadratic frequency dependence of the resistance of superconductors,

$$R_s \propto \omega^2. \quad (11)$$

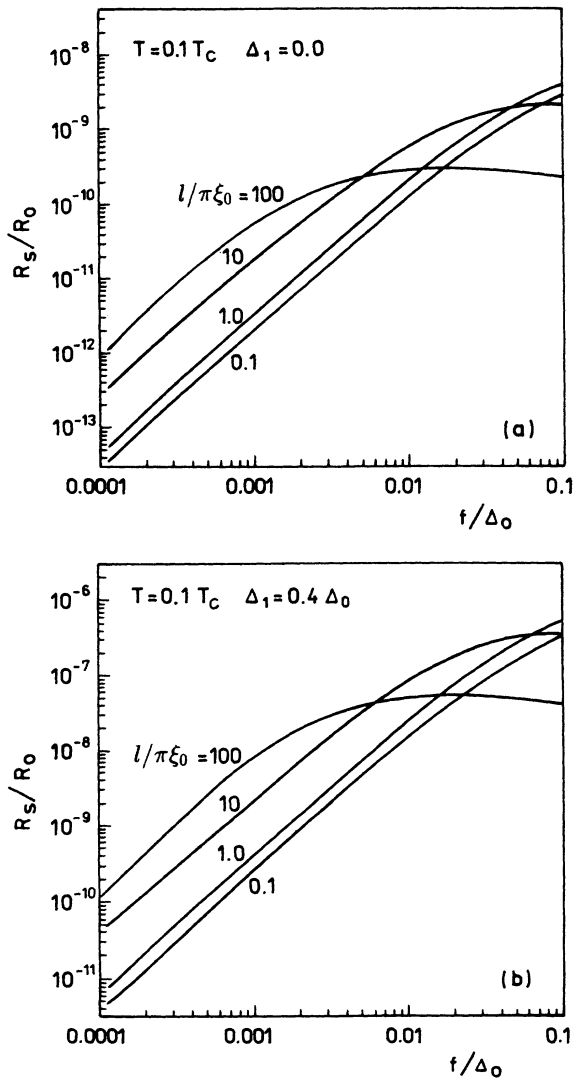


FIG. 6. Surface resistance  $R_s$  at very low frequencies at  $T=0.1T_c$  and (a)  $\Delta_1=0$ , (b)  $\Delta_1=0.4\Delta_0$ . Different curves correspond to different mean-free paths  $l/\pi\xi_0=1.0, 10.0$ , and  $100.0$ .

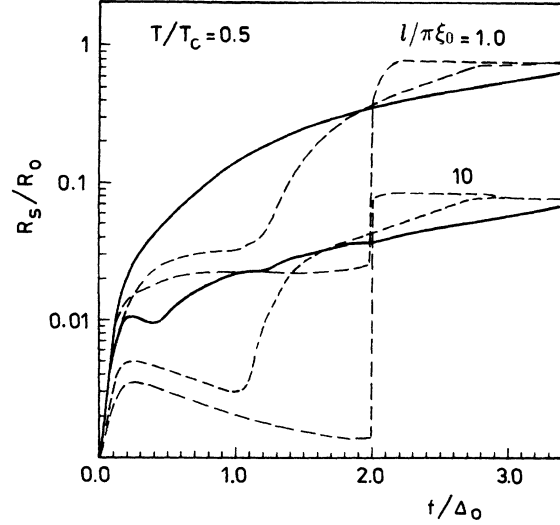


FIG. 7. Normalized surface resistance  $R_s$  as a function of frequency in the optical region at  $T=0.5T_c$  and for two values of mean-free path  $l$ . The long-dashed lines refer to the isotropic energy gap, the short-dashed lines to the anisotropic gap with  $\Delta_1/\Delta_0=0.4$ , and the solid curves to the anisotropic gap with  $\Delta_1/\Delta_0=0.8$ .

Figures 6(a) and 6(b) show that this behavior is also observed in systems with isotropic energy gap, and the value of the exponent (here  $\approx 2.0$ ), in fact, does not depend on the mean-free path  $l$ . It is interesting to note that the quadratic form (11) is found in classic Mattis-Bardeen<sup>2</sup> analysis and also for quite different models.<sup>6,8</sup> One can see that validity of (11) increases slightly with increasing gap anisotropy.

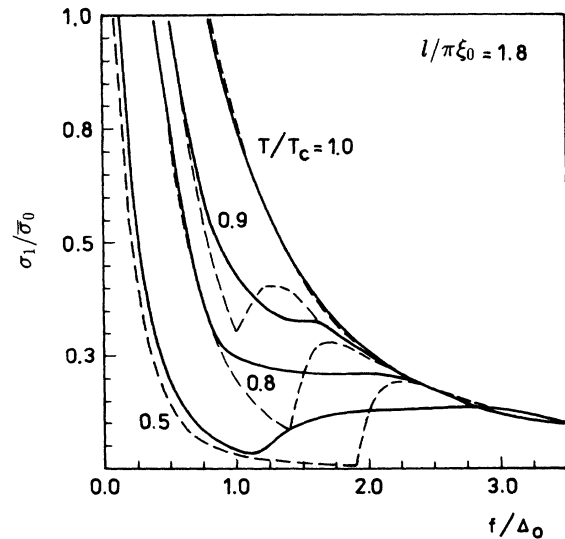


FIG. 8. The real part of conductivity  $\sigma_1$  normalized to  $\bar{\sigma}_0=ne^2/2m\Delta_0$  vs frequency in the optical region. The mean-free path  $l=1.8\pi\xi_0$ . Different curves correspond to different temperatures. The dashed lines refer to the isotropic energy gap and the solid ones to the moderately anisotropic gap with  $\Delta_1/\Delta_0=0.4$ .

#### D. Frequency dependence—optical region

Here we discuss results of our calculations for frequencies of the order of the energy gap  $\hbar\omega = \Delta_0$ . Figure 7 shows  $R_s$  plotted versus frequency in units of  $\Delta_0$  for two values of  $l$  and anisotropy parameter  $d_1 = 0, 0.4, 0.8$ . We choose two mean-free-path values  $l/\pi\xi_0 = 1$  and 10, which should cover the typical range for the high- $T_c$  superconductors. The long-dashed lines represent the isotropic  $\Delta$  characteristics. The short-dashed and solid curves refer to the anisotropic energy gap with  $\Delta_1/\Delta_0 = 0.4$  and  $\Delta_1/\Delta_0 = 0.8$ , respectively. Temperature  $T$  is equal to  $0.5T_c$ . In a system with short values of  $l$ , anisotropy influences the results so strongly that the  $R_s$  of the superconductor does not even demonstrate evidence of the energy gap. For longer  $l$ , the nonmonotonic dependence on  $\omega$  remains even for anisotropic materials, but it shows very complicated behavior especially for larger anisotropies.

Recently the frequency dependence of the conductivity of two-dimensional  $\text{CuO}_2$  sheets in the 1:2:3 phase has been measured<sup>26</sup> at different temperatures. The authors found that the various features of the  $\sigma(\omega)$  curves remained unchanged even though the experiments have been performed at temperatures  $T$  ranging from  $T \simeq 0$  up to  $T > T_c$ . Furthermore, they have concluded that this fact indicated  $T$  independence of the superconducting gap and thus “the phenomenology of dynamic properties [that] is fundamentally different from that of conventional superconductors.”

We have performed calculations of  $\sigma_1(\omega)$  with the parameters, which should be relevant for this experiment. Figure 8 shows the results. Dashed curves have been obtained for the case with isotropic  $\Delta$  and the solid lines for anisotropic energy gap with  $\Delta_1 = 0.4\Delta_0$ . The temperature dependence of  $\Delta$  has been taken in the BCS form in order to minimize non-BCS input, as already discussed [see Eq. (10)]. The sharp minimum of  $\sigma_1(\omega)$ , which moves to lower frequencies with increasing temperature and which traces the  $T$  dependence of  $\Delta$  for isotropic gap material broadens and shows no (or even opposite than expected)  $T$  dependence for weakly anisotropic gap. This behavior is very similar to that found experimentally.

Direct comparison of our results with experimental data<sup>26</sup> is perhaps not legitimate as we have not taken any phonon oscillators into considerations. These, however, should lead to even closer agreement between theory and experiment. Similar experiment has been performed by van der Marel *et al.*<sup>27</sup> These authors found that their re-

sults are in good agreement with the two-fluid model and in “strong disagreement with standard BCS theory.”

In our opinion, the gap anisotropy provides an alternative, and, in fact, more conventional explanation of these experimental data. Our finding does not invalidate non-standard interpretations, of course; it merely provides a simpler one based on the well-established picture of superconductivity.

#### IV. CONCLUSIONS

We have investigated the anisotropy of the layered superconductors and its influence on the finite-frequency electromagnetic properties of the two-dimensional superconducting systems. The anisotropy is understood here as the dependence of interactions and thus superconducting gap on the directions in the  $ab$  plane, as is usual in crystals (even with cubic or square symmetry) and not the anisotropy between  $a$  and  $b$  directions, which is small. Generally speaking, the anisotropy essentially does not change the surface reactance  $X_s$ .

We have calculated the effect of gap anisotropy on various characteristics of superconductors. None of the results obtained is in contradiction with existing experimental data. Moreover, in a few cases our calculations seem to show the trends which fit those observed experimentally, in particular, the frequency dependence of  $R_s$  at low  $\omega$  and  $T$  remains quadratic in accord with other calculations and with experiment; the temperature dependence of  $R_s$  at moderate values of  $T$  [Fig. 3(b)] obtained for anisotropic materials has, similarly as experimental data, much lower slope than the one found for isotropic gap; calculated  $T$  dependence of the London penetration depth (not presented in this paper) only weakly changes with gap anisotropy; and  $\sigma_1(\omega, T)$  curves (Fig. 8) strongly resemble the experimental data<sup>26,27</sup> and offer their novel, though more classic, interpretation.

In conclusion, the anisotropy of the gap is an important factor, which strongly modifies the behavior of some characteristics of superconductors. It thus has to be taken into consideration in the interpretation of experimental data.

#### ACKNOWLEDGMENTS

This work has been partially supported by the KBN under Contract No. 20 285 9101/91-92/. We thank Professor R. Micnas and Professor S. Robaszkiewicz for discussions and for calling our attention to Ref. 26.

<sup>1</sup>J. Bardeen, L. N. Cooper, and J. R. Schrieffer, *Phys. Rev.* **108**, 1175 (1957).

<sup>2</sup>D. C. Mattis and J. Bardeen, *Phys. Rev.* **111**, 412 (1958).

<sup>3</sup>J. G. Bednorz and K. A. Müller, *Z. Phys. B* **64**, 189 (1986).

<sup>4</sup>H. Ebisawa, Y. Isawa, and S. Maekawa, *Jpn. J. Appl. Phys.* **26**, L992 (1987).

<sup>5</sup>J. J. Chang and D. J. Scalapino, *Phys. Rev. B* **40**, 4299 (1989).

<sup>6</sup>V. Z. Kresin, *J. Supercond.* **3**, 177 (1990).

<sup>7</sup>R. A. Klemm, K. Scharnberg, D. Walker, and C. T. Rieck, *Z.*

*Phys. B* **72**, 139 (1989).

<sup>8</sup>D. Walker and K. Scharnberg, *J. Supercond.* **3**, 269 (1990).

<sup>9</sup>D.M.T. Kuo and P. M. Hui, *Physica C* **174**, 365 (1991).

<sup>10</sup>Y. R. Wang, M. J. Rice, and C. B. Duke, *Phys. Rev. B* **37**, 9869 (1988).

<sup>11</sup>T. M. Rice and F. C. Zhang, *Phys. Rev. B* **39**, 815 (1988); S. T. Chui, R. V. Kasowski, and W. Y. Hsu, *Phys. Rev. Lett.* **61**, 885 (1988).

<sup>12</sup>N. E. Bickers, D. J. Scalapino, R. T. Collins, and Z. Schles-

- inger, Phys. Rev. B **42**, 67 (1990).
- <sup>13</sup>G. A. Thomas *et al.*, Phys. Rev. Lett. **61**, 1313 (1988).
- <sup>14</sup>T. Timusk *et al.*, Phys. Rev. B **38**, 6683 (1988).
- <sup>15</sup>Z. Schlesinger *et al.*, Phys. Rev. B **41**, 11 237 (1990).
- <sup>16</sup>W. Bauhofer *et al.*, Phys. Rev. Lett. **63**, 2520 (1989).
- <sup>17</sup>L. Drabeck *et al.*, Phys. Rev. B **39**, 785 (1989).
- <sup>18</sup>D. Kalokitis *et al.*, J. Electron. Mater. **19**, 117 (1990).
- <sup>19</sup>H. Krenn *et al.*, Phys. Rev. B **39**, 6716 (1989).
- <sup>20</sup>D. R. Harshman *et al.*, Phys. Rev. B **39**, 851 (1989).
- <sup>21</sup>L. Krusin-Elbaum *et al.*, Phys. Rev. Lett. **62**, 217 (1989).
- <sup>22</sup>S. L. Cooper and M. V. Klein, Comments Condens. Mater. Phys. **15**, 99 (1990).
- <sup>23</sup>A. Zibold *et al.*, Physica C **171**, 151 (1990).
- <sup>24</sup>D. W. Cooke, E. R. Gray, P. N. Arendt, J. G. Beery, B. L. Bennett, D. R. Brown, R. J. Houlton, M. S. Jahan, A. J. Klapetzky, M. A. Maez, I. D. Raistrick, G. A. Reeves, and B. Rusnak (unpublished).
- <sup>25</sup>D. W. Cooke *et al.*, Solid State Commun. **73**, 297 (1990).
- <sup>26</sup>R. T. Collins *et al.*, Phys. Rev. B **43**, 8701 (1991).
- <sup>27</sup>D. van der Marel *et al.*, Phys. Rev. B **43**, 8606 (1991).
- <sup>28</sup>G. M. Eliashberg, Zh. Eksp. Teor. Fiz. **38**, 966 (1960) [Sov. Phys. JETP **11**, 696 (1960)].
- <sup>29</sup>S. B. Nam, Phys. Rev. **156**, 470 (1967); **156**, 487 (1967).
- <sup>30</sup>F. Marsiglio, J. P. Carbotte, and J. Blezius, Phys. Rev. B **41**, 6457 (1990).
- <sup>31</sup>F. Marsiglio and J. P. Carbotte, Phys. Rev. B **41**, 11 114 (1990).
- <sup>32</sup>L. A. Falkowsky and S. Klama, Physica C **172**, 242 (1990).
- <sup>33</sup>G. D. Mahan, Phys. Rev. B **39**, 11 317 (1989).
- <sup>34</sup>K. I. Wysokiński and T. Dziura, Solid State Commun. **76**, 383 (1990).
- <sup>35</sup>G. Rickayzen, *Theory of Superconductivity* (Wiley, New York, 1965).
- <sup>36</sup>K. Scharnberg, J. Low Temp. Phys. **30**, 229 (1978).
- <sup>37</sup>See, e.g., B. Batlogg, in *High Temperature Superconductivity*, Proceedings of the Los Alamos Symposium, 1989, edited by K. Bedel, D. Coffey, D. Meltzer, D. Pines, and J. R. Schrieffer (Addison-Wesley, Reading, MA, 1990).
- <sup>38</sup>M. A. Biondi, M. P. Garfunkel, and W. A. Thomson, Phys. Rev. **136**, A1471 (1964).
- <sup>39</sup>J. R. Clem, Ann. Phys. (N.Y.) **40**, 269 (1966).